

Urbanization effects on vegetation cover in major African cities during 2001–2017

Rui Yao^a, Jin Cao^b, Lunche Wang^{a,*}, Wenwen Zhang^a, Xiaojun Wu^a

^a Laboratory of Critical Zone Evolution, School of Earth Sciences, China University of Geosciences, Wuhan 430074, China

^b Faculty of Resources and Environmental Science, Hubei University, Wuhan 430062, China

ARTICLE INFO

Keywords:

Urbanization
Vegetation
Remote sensing
Enhanced vegetation index
Africa

ABSTRACT

Urbanization effects on vegetation cover (VC) have been analyzed in many regions. However, little attention has been paid to Africa, which has undergone rapid urbanization in recent decades. In this study, MODIS land cover and enhanced vegetation index (EVI) data were used to examine urbanization effects on VC in 59 large cities in Africa during 2001–2017. The Δ EVI (urban EVI minus rural EVI) was used to represent urbanization effects on VC. Major findings include: (1) for 59 cities averaged, annual Δ EVI averaged from 2015 to 2017 was -0.116. Negative annual Δ EVI (i.e. urban EVI lower than rural) were observed in 56 of 59 cities. (2) For 59 cities averaged, urban area increased 17.9% from 2001 (262.8 km²) to 2016 (309.8 km²). (3) Annual Δ EVI decreased significantly ($p < 0.05$) in 44 of 59 cities for the period 2001–2017, and annual average area of urbanization effects on VC increased significantly in 40 of 59 cities. For 59 cities averaged, the percentage of urban area with significant decreasing trends of annual Δ EVI was 60.0%. Spatially, cities near the Gulf of Guinea showed more significant decreasing Δ EVI than cities in other regions. In addition, the trends and spatial distributions of urbanization effects on VC differed little by seasons. These results suggested that urbanization and its effects on VC in Africa should arouse more attentions.

1. Introduction

Vegetation is an important component of terrestrial ecosystems. It is essential for life on earth and provides a plethora of benefits to humans and the environment. For example, vegetation can absorb atmospheric CO₂ helping to mitigate the green house effects (Davies et al., 2011; Myeong et al., 2006). In addition, vegetation can retain the precipitation thus prevent water and soil loss (Oldfield et al., 2013; Zhang et al., 2004a). Furthermore, urban vegetation can help to alleviate urban heat island through increasing shade and transpiration (Yao et al., 2017b; Zhou et al., 2017; Doick et al., 2014). Additionally, vegetation can mitigate air pollution through absorbing O₃, PM₁₀, NO₂, SO₂ and CO (Nowak et al., 2006; Salmond et al., 2013). Finally, plant can alleviate noise pollution, since plant leaf can uptake acoustic energy (Fang and Ling, 2003; Pathak et al., 2008).

Unfortunately, urbanization can significantly decrease vegetation cover (VC) through transforming land cover types from vegetated areas to built-up areas. This issue is especially serious in recent decades, when the speed of urbanization was unseen in human's history (Vitousek et al., 1997; Foley et al., 2005). The urbanization effects on VC have been systematically investigated in Europe, Asia and North America

(Chen et al., 2017; Dallimer et al., 2011; Nowak and Greenfield, 2012; Yang et al., 2014; Yao et al., 2017a; Zhao et al., 2013; Zhou et al., 2014). For example, Dallimer et al. (2011) used Landsat-based enhanced vegetation index (EVI, a proxy for VC) to study the urban greenspaces in England. Their results showed that urban greenspaces decreased in 9 of 13 cities in England during 2000–2008. Zhou et al. (2014) used the Δ EVI (urban EVI minus rural) to reflect the urbanization effects on VC and showed that the Δ EVI decreased significantly in over half of the 32 cities in China for the period 2000–2012. Nowak and Greenfield (2012) showed that the urban tree cover decreased significantly in 17 out of 20 cities in United States. However, little attention has been paid to Africa. To our knowledge, few studies have analyzed the urbanization effects on VC for a large area in Africa. Liu et al. (2015) found that the urbanization effects on VC differed largely by 50 global large cities. But Liu et al. (2015) only investigated two African cities. Megahed et al. (2015) used Landsat TM and OLI data to study land cover change in Cairo (Egypt). It was found that 13% of the vegetated area transformed to urban area from 1984 to 2003, and a further 12% of the vegetated area transformed to urban area during 2003 to 2014. Using Landsat MSS and TM data, Nwaogu et al. (2017) found that VC in Onitsha (Nigeria) decreased from 1987 to 2015. Using

* Corresponding author.

E-mail address: wang@cug.edu.cn (L. Wang).

<https://doi.org/10.1016/j.jag.2018.10.011>

Received 3 August 2018; Received in revised form 12 October 2018; Accepted 16 October 2018

Available online 30 October 2018

1569-8432/ © 2018 Elsevier B.V. All rights reserved.

Landsat ETM + data, Coulter et al. (2016) showed an increase in built-up areas but a reduction in forest in Kumasi and Accra (Ghana) from 2000 to 2010. Different studies used different data and methods to assess the urbanization effects on VC for different time periods, their results were not comparable. Thus urbanization effects on VC were poorly understood in Africa.

Africa has experienced rapid urbanization in past decades. Urban population accounted for 31.5% of the total population in 1990 but 41.2% in 2015 in Africa (United Nations, 2014). Comparatively, urban population in Europe accounted for 69.9% and 73.9% of the total population in 1990 and 2015, respectively (United Nations, 2014). The proportion of urban population to total population in Africa was much lower than developed areas, but the increasing rate of the proportion was much faster than developed areas. In addition, urban population in Africa was 32.7 million, 82.6 million, 200.1 million and 408.6 million in 1950, 1970, 1990 and 2010, respectively (United Nations, 2014). Thus the urbanization effects on VC in Africa should be comprehensively studied, which has not been documented in literature. To fill this research gap, this study aims at: (1) revealing the urbanization effects on VC in 59 African large cities; (2) examining urbanization in Africa; and (3) analyzing the trends of urbanization effects on VC in Africa.

2. Data and methods

2.1. Study area

Africa's land area is approximately 30.2 million km², which is the second largest continent in the world and accounts for about 20.3% of the world's total land area (Fig. 1). The area with average annual temperature above 20 °C accounts for about 90.2% of the total area (climate data was derived from Climatic Research Unit (CRU) TS4.01 dataset, hereafter (Harris et al., 2014)). The average annual total precipitation in approximately one-third of the total continents is less than 200 mm. Precipitation in Africa decreases from the equator to the north and south. For example, the average precipitation in the latitude range of ± 10° is about 1230 mm, while in other area is approximately 415 mm. The distribution of precipitation is similar to EVI (latitude range of ± 10°: 0.35; other areas: 0.16). In this study, we choose 59 cities with urban area higher than 100 km² (see Section 2.2). Detailed information (e.g. city name, country, latitude, longitude and urban area) of the 59 African.

2.2. Data

In this study, Moderate-resolution Imaging Spectroradiometer (MODIS) land cover data (MCD12Q1, version 6, IGBP classification layer, yearly composite, 500 m spatial resolution, a total of 42 tiles) in the year 2001 and 2016 (the latest year available when the manuscript is finished) was used to extract land cover information in Africa (Menashe and Friedl, 2018). In addition, vegetation greenness information in Africa from 2001 to 2017 was derived from MOD13A3 EVI data (version 6, EVI layer, monthly composite, approximately 1000 m spatial resolution, a total of 42 tiles) (Yao et al., 2018a; Zhang et al., 2017; Huete et al., 2002).

2.3. Methods

The MCD12Q1 data was first resampled to 1000 m spatial resolution to match the MOD13A3 EVI data. Then we extracted urban areas and water bodies from MCD12Q1 data (urban area: pixel with digital number equal to 13; water bodies: pixel with digital number equal to 17 (Menashe and Friedl, 2018)). In the present study, cities with urban area higher than 100 km² in the year 2016 were selected as study areas (Fig. 1). In addition, 20–25 km buffers around the urban areas were generated and used as reference rural areas after excluding water bodies and other urban areas (Yao et al., 2018b, b; Zhou et al., 2016).

We did not use the buffers near the urban areas since the footprint of urbanization tend to be larger than actual urban area (Han and Xu, 2013; Liu et al., 2015; Zhang et al., 2004b). To examine the urbanization in Africa, the urban areas in 59 African cities in the year 2016 were compared with 2001 (Section 3.2). Urban areas in 2016 were used to reveal urbanization effects on VC for the period 2001–2017 (Section 3.1 and 3.3).

Annual and seasonal average (March–April–May (MAM, northern hemisphere spring or southern hemisphere autumn), June–July–August (JJA, northern hemisphere summer or southern hemisphere winter), September–October–November (SON, northern hemisphere autumn or southern hemisphere spring), December–January–February (DJF, northern hemisphere winter or southern hemisphere summer)) EVIs were first calculated for each pixel in this study. In addition, the Δ EVI was used to represent the urbanization effects on VC (Peng et al., 2012; Yao et al., 2017a; Zhou et al., 2014):

$$\Delta\text{EVI} = \text{EVI}_{\text{urban}} - \text{EVI}_{\text{rural}} \quad (1)$$

where the $\text{EVI}_{\text{urban}}$ and $\text{EVI}_{\text{rural}}$ represent the EVI in urban and rural areas (spatial average), respectively.

In the present study, the urbanization effects on VC were analyzed using three indicators:

- (1) Δ EVI. The spatial characteristics of Δ EVI averaged from 2015 to 2017 were first analyzed (section 3.1). Then the trends of Δ EVI during 2001–2017 were calculated using linear regression analyses for each city individually (section 3.3).
- (2) Area of urbanization effects on VC. In each city, pixel meeting the following requirements was considered that the VC has been affected by urbanization: 1) in urban area or 10 km buffer around the urban area and 2) EVI lower than rural mean EVI minus standard deviation of rural EVI (all pixels in the 20–25 km buffer of a city) (Ward et al., 2016; Yao et al., 2017b; Zhang and Wang, 2008). The pixels in 10 km buffer around the urban area were also included because the footprint of urbanization may be larger than urban area (Han and Xu, 2013; Liu et al., 2015; Zhang et al., 2004b). The standard deviation segmenting method may reduce uncertainties caused by arbitrarily selected threshold (Zhang and Wang, 2008). The area of urbanization effects on VC was calculated as the total area of all pixels that meet the two requirements in a city. The spatial and seasonal variations of the area of urbanization effects on VC averaged from 2015 to 2017 were first analyzed (Section 3.1). In addition, the trends of area of urbanization effects on VC in each city for the period 2001–2017 were calculated using linear regression analyses (Section 3.3).
- (3) Percentage of urban area with decreasing Δ EVI. Firstly, for each urban pixel, we calculated the Δ EVI (EVI in one urban pixel minus rural mean EVI) and then computed the trends of Δ EVI during 2001–2017 using linear regression analyses. Then the urban area with decreasing Δ EVI was calculated as the total area of all urban pixels with decreasing Δ EVI (linear changing rate of Δ EVI lower than zero). Finally, the percentage of urban area with decreasing Δ EVI was calculated as dividing the urban area with decreasing Δ EVI by the total urban area of the city (Section 3.3).

3. Results and discussion

3.1. Spatial and seasonal variations of urbanization effects on VC

The spatial distributions of Δ EVI averaged from 2015 to 2017 were illustrated in Fig. 2. The Δ EVI averaged from 2015 to 2017 in each city. For 59 cities averaged, annual Δ EVI was -0.116, whose absolute value was more than twice as much as the standard deviation of urban EVI of 59 cities (0.049). This suggested that the rural EVI was significantly higher than urban EVI. Spatially, annual Δ EVI differed greatly by cities,

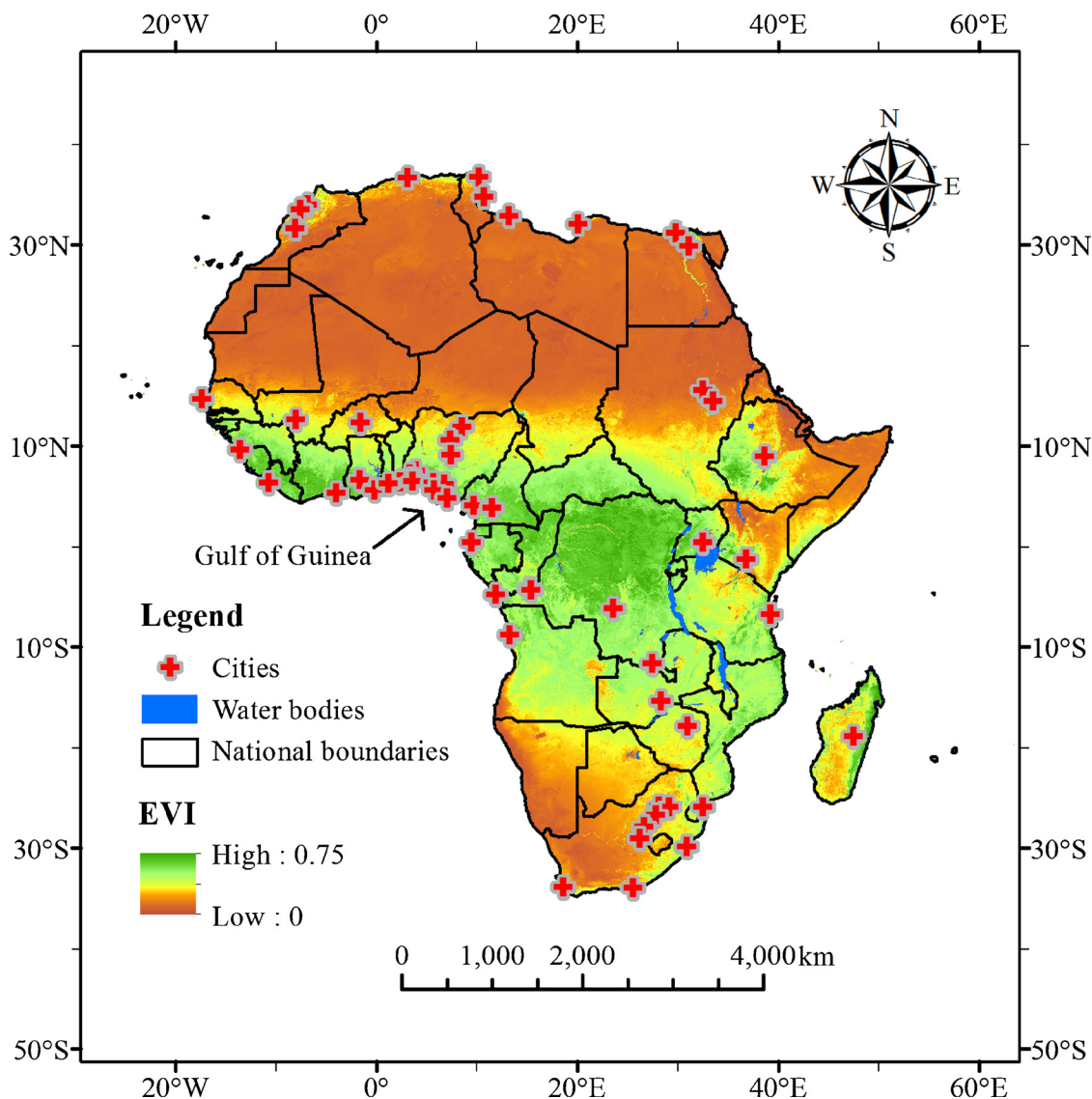


Fig. 1. Study area in this study. Red crosses represent selected cities. The background map is mean annual enhanced vegetation index (EVI) during 2001–2017. (For interpretation of the references to colour in this figure legend, the reader is referred to the web version of this article).

the lowest and highest annual ΔEVI were -0.247 (Abidjan (Coate d'Ivoire)) and 0.010 (Khartoum (Sudan)), respectively. Negative annual ΔEVI s were observed in 56 of 59 cities. Only 3 cities (Sfax (Tunisia), Marrakech (Morocco), Khartoum (Sudan)) in desert area exhibited positive annual ΔEVI . In addition, cities near the Gulf of Guinea generally showed lower ΔEVI than cities in other regions (Fig. 2). For example, if we defined the 19 cities in Nigeria, Ghana, Togo, Cameroon and Gabon as cities near the Gulf of Guinea (Fig. 2), the annual ΔEVI averaged for these 19 cities was -0.167. This may be attributed to: (1) stabler urban EVI than rural EVI (standard deviation (annual): 0.049 vs. 0.102) across cities; and (2) high background rural EVI in this region (0.391). We showed that the spatial variations in annual ΔEVI were strongly dependent on background annual rural EVI (Pearson's correlation analyses (hereafter): $r = -0.896$, $p < 0.01$). Seasonally, the spatial distributions and means of ΔEVI were similar across seasons. The ΔEVI s averaged for 59 cities were -0.128, -0.110, -0.113 and -0.113 in MAM, JJA, SON and DJF, respectively. These may be attributed to two main reasons. Firstly, many African cities were near the equator, the rural EVI is high and the ΔEVI is low throughout a year. Secondly, certain cities away from the equator were generally surrounded by sparse vegetated areas (Fig. 1), thus they showed lower rural EVI and higher ΔEVI across seasons. For example, there are 29 cities in the

latitude range of $\pm 10^\circ$. For these 29 cities averaged, the rural EVI for 4 seasons ranged from 0.337 to 0.418. The range is from 0.205 to 0.266 for other 30 cities averaged.

The area of urbanization effects on VC averaged from 2015 to 2017 was shown in Fig. 3. For 59 cities combined, annual area of urbanization effects on VC averaged from 2015 to 2017 was 556.4 km², ranging from 0 (Cairo (Egypt)) to 3145.3 km² (Johannesburg (South Africa)). The annual area of urbanization effects on VC averaged from 2015 to 2017 was significantly and positively correlated with urban area in the year 2016 ($r = 0.794$, $p < 0.01$). In addition, a weak but statistically significant correlation between annual area of urbanization effects on VC and annual rural EVI was found ($r = 0.320$, $p < 0.05$). Furthermore, the spatial and seasonal variations of area of urbanization effects on VC averaged from 2015 to 2017 were generally consistent with ΔEVI (Fig. 3). The 19 cities near the Gulf of Guinea generally showed large area of urbanization effects on VC (19 cities averaged: 668.7 km²). The areas of urbanization effects on VC were 571.6, 552.9, 492.2 and 553.3 km² in MAM, JJA, SON and DJF, respectively. Overall, these results suggested that urbanization has had a great impact on VC in most African cities, especially for cities near the Gulf of Guinea.

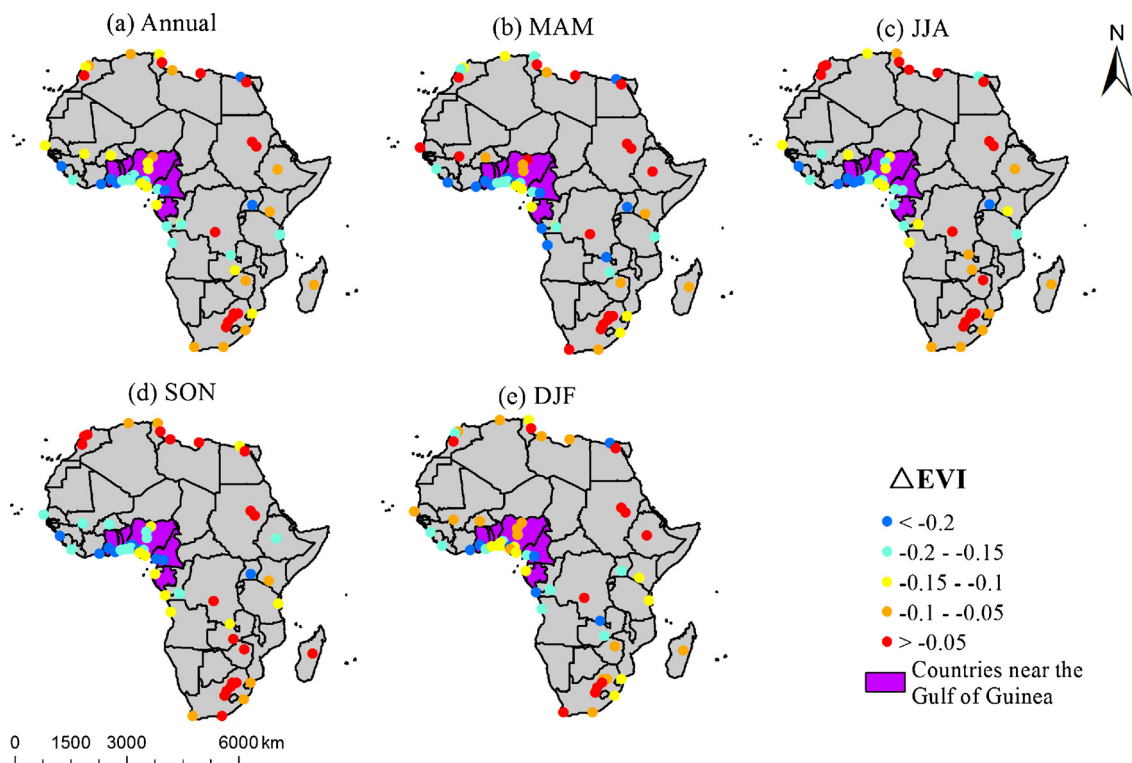


Fig. 2. Spatial and seasonal variations in ΔEVI in 59 African cities during 2015–2017. MAM: March–April–May, JJA: June–July–August, SON: September–October–November, DJF: December–January–February.

3.2. Urbanization from 2001 to 2016

The spatial distributions of urban area change in 59 African cities from 2001 to 2016 are illustrated in Fig. 4. The urban area change in each city. Urban area increased in 57 of 59 cities from 2001 to 2016.

Only two cities (Sfax (Tunisia) and Mbuji-Mayi (Congo)) exhibited the same urban area between 2001 and 2016. We utilized 30 m spatial resolution Landsat data to further examine urbanization in these two cities. The same urban area between 2001 and 2016 derived from MCD12Q1 data may be attributed to: (1) slow urbanization in these two

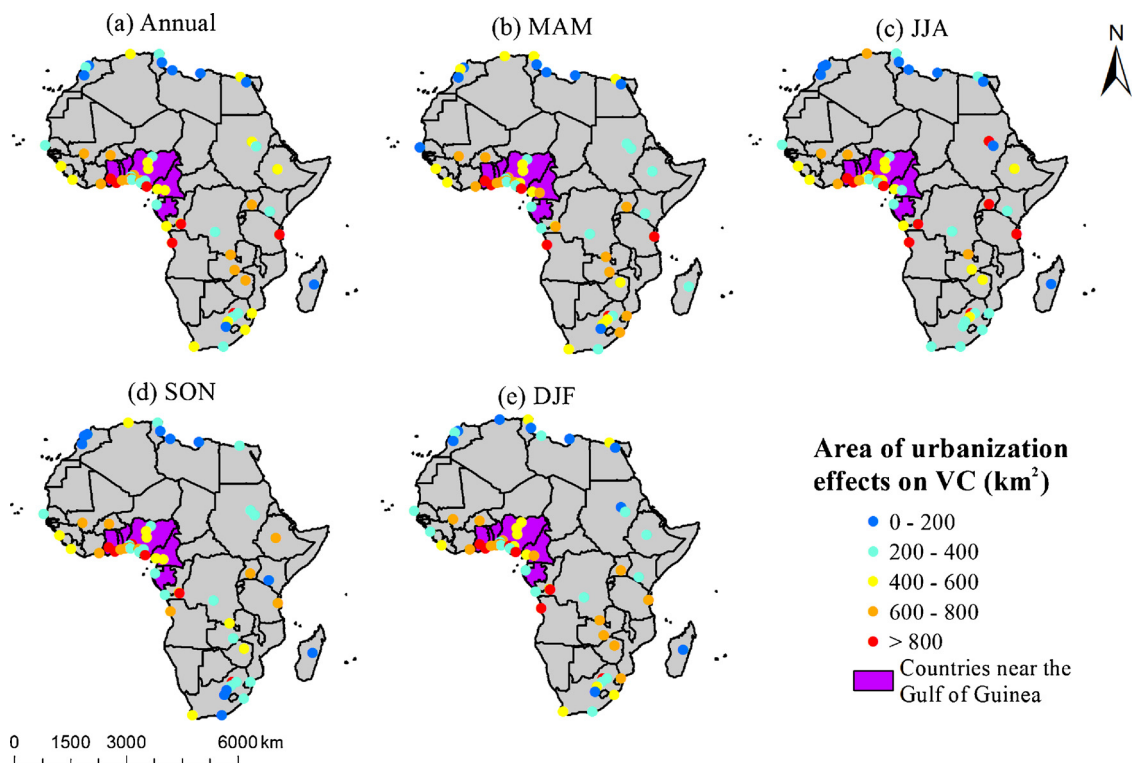


Fig. 3. Spatial and seasonal variations of the area of urbanization effects on vegetation cover (VC) in 59 African cities during 2015–2017.

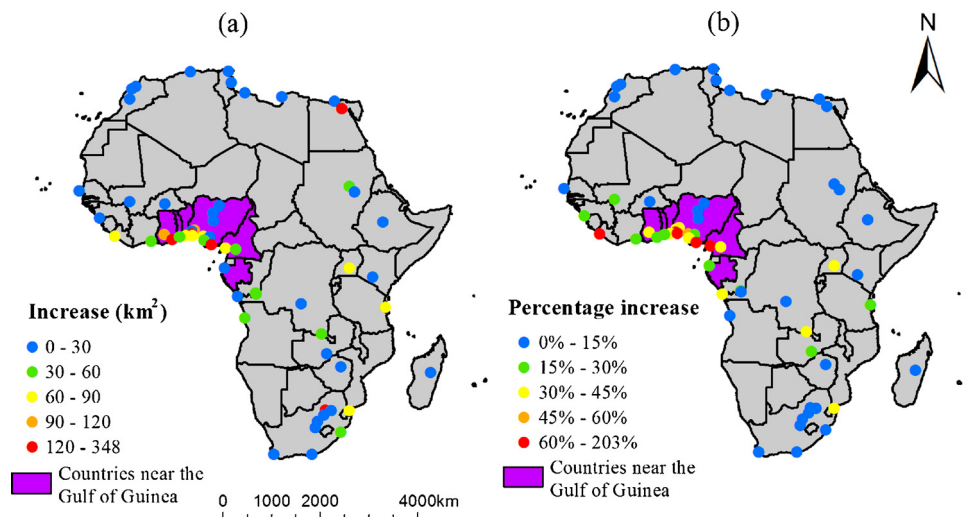


Fig. 4. Urbanization in 59 African cities from 2001 to 2016 as revealed by MCD12Q1 data: (A) urban area difference between 2001 and 2016; (B) percentage increase in urban area.

cities from 2001 to 2016; (2) relative low accuracy of MCD12Q1 data (Figs. S1 and S2). For 59 cities averaged, urban area increased from 262.8 km² in 2001 to 309.8 km² in 2016. City with the fastest growth in urban area was Lagos (Nigeria) (from 541.9 km² in 2001 to 884.1 km² in 2016). In addition, cities with faster growth of urban area were mainly concentrated in the region near the Gulf of Guinea (19 cities averaged: 87.31 km²). Furthermore, the increase in urban area from 2001 to 2016 was significantly and positively correlated with urban area in 2001 ($r = 0.362$, $p < 0.01$). Thus cities with larger urban area in 2001 may show greater increase in urban area during 2001–2016.

Percentage change in urban area from 2001 to 2016 was also analyzed (Fig. 4b). For 59 cities averaged, urban area increased 17.9% from 2001 to 2016. City with the highest percentage increase in urban area was Ikorodu (Nigeria, 203.3%, from 77.3 km² in 2001 to 234.4 km² in 2016). Cities in the Gulf of Guinea generally showed higher percentage increase in urban area than cities in other region (19 cities averaged: 28.7%). In addition, the percentage increase in urban area from 2001 to 2016 was insignificantly correlated with urban area in 2001 ($r = -0.132$, $p = 0.320$).

3.3. Trends of urbanization effects on VC during 2001–2017

3.3.1. Trends of EVI and Δ EVI during 2001–2017

The Δ EVI decreased significantly ($p < 0.05$) in most cities for the period 2001–2017 (Fig. 5). Annual Δ EVI decreased significantly in 44 of 59 cities (Table 1). The highest decreasing rate of annual Δ EVI was observed in Ikorodu (Nigeria, $-0.0081/\text{year}$, $p < 0.01$), while the highest increasing rate of annual Δ EVI was found in Mbuji-Mayi (Congo, $0.0024/\text{year}$, $p < 0.01$). As mentioned in Section 3.2, Mbuji-Mayi showed slow urbanization (the same urban area between 2001 and 2016), thus little vegetation is affected by urbanization. Additionally, in Mbuji-Mayi, annual urban EVI increased significantly during 2001–2017 ($0.00213/\text{year}$, $p < 0.01$), while rural EVI was stable (-0.00025 , $p > 0.05$). Thus the significant increasing trend of Δ EVI in Mbuji-Mayi may be related to the urban greening policies. For 59 cities averaged, the annual Δ EVI decreased at the rate of $-0.00268 \pm 0.00208/\text{year}$ (mean and standard deviation, hereafter) (Table 2). In addition, the trends of Δ EVI differed little by seasons. The numbers of cities with significant decreasing trends of Δ EVI in MAM, JJA, SON and DJF were 43, 35, 35 and 43, respectively (Table 1). The trends of Δ EVI decreased at the rate of $-0.00282 \pm 0.00250/\text{year}$, $-0.00257 \pm 0.00222/\text{year}$, $-0.00270 \pm 0.00264/\text{year}$ and $-0.00265 \pm 0.00295/\text{year}$ in MAM, JJA, SON and DJF, respectively (Table 2). Finally, most cities near the Gulf of Guinea showed

significant decreasing trends of Δ EVI (19 cities averaged: $-0.00462/\text{year}$).

The urban EVI decreased significantly in most cities during 2001–2017 (Fig. 6). Annual urban EVI decreased significantly in 41 of 59 cities (Table 1). The highest decreasing rate of annual urban EVI was observed in Ikorodu (Nigeria, $-0.0081/\text{year}$, $p < 0.01$), while the highest increasing rate of annual urban EVI was found in Mbuji-Mayi (Congo, $0.00213/\text{year}$, $p < 0.01$). For 59 cities averaged, the annual urban EVI decreased at the rate of $-0.00257 \pm 0.00243/\text{year}$ (Table 2). As mentioned above, annual Δ EVI decreased at the rate of $-0.00268 \pm 0.00208/\text{year}$, thus the decreased Δ EVI can primarily be attributed to decreased urban EVI. In addition, the spatial and seasonal variations in urban EVI tend to similar with Δ EVI (Fig. 6 and Table 2).

Most cities showed insignificant trends of rural EVI during 2001–2017 (Fig. 7). Insignificant trends of annual rural EVI were observed in 49 of 59 cities (Table 1). Significant positive and negative trends of annual rural EVI were found in only 7 and 3 cities, respectively. In addition, annual rural EVI increased at the rate of $0.00012 \pm 0.00093/\text{year}$ averaged for 59 cities (Table 2). The highest and lowest changing rates of annual rural EVI were observed in Algiers (Algeria, $0.00197/\text{year}$ ($p < 0.05$)) and Port Harcourt (Nigeria, $-0.00293/\text{year}$ ($p < 0.01$)), respectively. Finally, trends of rural EVI did not show significant spatial and seasonal variations (Fig. 7 and Table 2). The insignificant trend of rural EVI was different from previous studies, which showed that the earth is greening (Zhu et al., 2016; Zeng et al., 2017). This was possibly because the study period (17 years) in this study is much short than previous studies (approximately 30 years) (Table 3).

Yao et al., (2018a) showed that the interannual standard deviation of EVI was generally lower in urban than in rural areas, since EVI was much lower in urban than in rural areas. Thus the decreasing Δ EVI may be attributed to higher increasing rate of rural EVI than in urban EVI, especially in the context of global greening (Zhang et al., 2017). That is one of the reasons why we further analyzed urban and rural EVI separately. In this study, insignificant trends of rural EVI were found in 49 of 59 cities. The number of cities with significant decreasing trends of annual Δ EVI for the period 2001–2017 was 44. Among them, there are 34 cities showed significant decreasing trends of annual urban EVI and insignificant trends of annual rural EVI. Overall, these results suggested that the significant decreasing trends of Δ EVI during 2001–2017 can primarily be attributed to the reductions in urban EVI and stable rural EVI in most African cities. In addition, urbanization may play an important role in it. Finally, the results of this study were similar to previous studies, which examined the land use/land cover change at local

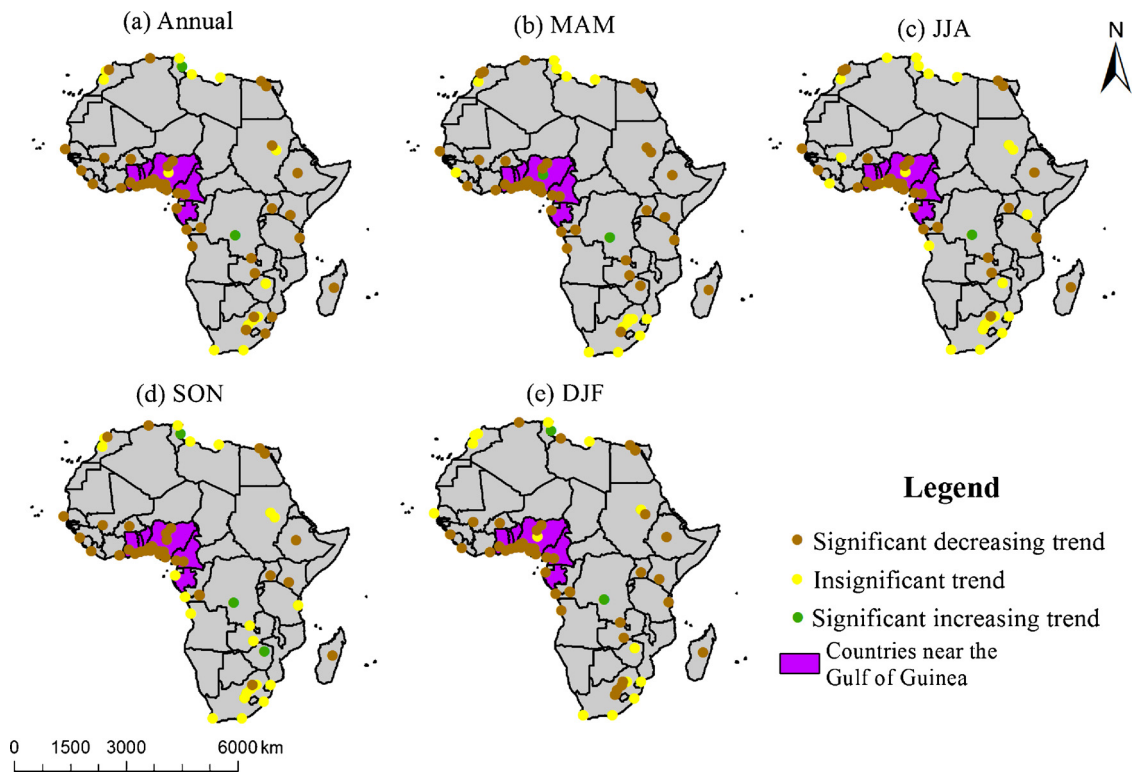


Fig. 5. Spatial distribution of trends of Δ EVI in 59 African cities from 2001 to 2017.

Table 1

Trends of enhanced vegetation index (EVI) and Δ EVI in 59 African cities from 2001 to 2017. The numbers of cities with increasing and decreasing trends of Δ EVI were listed at left and right, respectively. The numbers of cities with significant ($p < 0.05$) trends of Δ EVI were shown in the brackets. MAM: March–April–May, JJA: June–July–August, SON: September–October–November, DJF: December–January–February.

	Annual	MAM	JJA	SON	DJF
Δ EVI	3(2), 56(44)	5(2), 54(43)	5(1), 54(35)	8(3), 51(35)	3(2), 56(43)
Rural EVI	36(7), 23(3)	31(4), 28(0)	28(5), 31(6)	35(1), 24(7)	42(9), 17(1)
Urban EVI	9(4), 50(41)	7(3), 52(39)	11(2), 48(40)	9(2), 50(39)	7(5), 52(41)

scales. Previous studies showed that the urbanization significantly occupied vegetated area in Cairo (Egypt), Kumasi (Ghana), Accra (Ghana) and Onitsha (Nigeria) (Megahed et al., 2015; Nwaogu et al., 2017; Coulter et al., 2016). This study showed that the urban EVI and Δ EVI decreased significantly in all these four cities.

3.3.2. Trends of area of urbanization effects on VC for the period 2001–2017

The area of urbanization effects on VC increased in most African cities (Fig. 8). The changing rate of area of urbanization effects on VC. Annual area of urbanization effects on VC increased significantly 40 of 59 African cities. For 59 cities averaged, annual average area of

Table 2

Temporal trends of EVI and Δ EVI averaged (mean and standard deviation, hereafter) for 59 African cities from 2001 to 2017 (unit: 10^{-3} /year).

	Annual	MAM	JJA	SON	DJF
Δ EVI	-2.68 ± 2.08	-2.82 ± 2.50	-2.57 ± 2.22	-2.7 ± 2.64	-2.65 ± 1.95
Rural EVI	0.12 ± 0.93	0.20 ± 1.30	-0.31 ± 1.46	-0.11 ± 1.31	0.68 ± 1.15
Urban EVI	-2.57 ± 2.43	-2.62 ± 2.59	-2.88 ± 3.09	-2.81 ± 2.82	-1.97 ± 1.90

urbanization effects on VC increased at the rate of $9.7 \pm 9.6 \text{ km}^2/\text{year}$, ranging from $42.9 \text{ km}^2/\text{year}$ ($p < 0.01$) in Johannesburg (South Africa) to $-7.7 \text{ km}^2/\text{year}$ ($p < 0.01$) in Mbuji-Mayi (Congo). Additionally, most cities near the Gulf of Guinea witnessed significant increasing trends of annual area of urbanization effects on VC (19 cities averaged: $13.85 \text{ km}^2/\text{year}$). Furthermore, the area of urbanization effects on VC differed little by seasons (Table 4). The spatial distributions of area of urbanization effects on VC were similar across seasons (Fig. 8). Finally, the trends of area of urbanization effects on VC during 2001–2017 were significantly and positively correlated with the increase in urban area from 2001 to 2016 (annual: $r = 0.631$, $p < 0.01$; MAM: $r = 0.645$, $p < 0.01$; JJA: $r = 0.545$, $p < 0.01$; SON: $r = 0.581$, $p < 0.01$; DJF: $r = 0.669$, $p < 0.01$). The correlations between trends of area of urbanization effects on VC and the increase in urban area were stronger than between Δ EVI (annual: $r = -0.519$, $p < 0.01$; MAM: $r = -0.477$, $p < 0.01$; JJA: $r = -0.489$, $p < 0.01$; SON: $r = -0.463$, $p < 0.01$; DJF: $r = -0.420$, $p < 0.01$) (Fig. 9).

3.3.3. Percentage of urban area with decreasing Δ EVI

For 59 African cities averaged, significant increasing and decreasing trends of annual Δ EVI were observed in 60% and 4.6% of the urban area, for the period 2001–2017. The highest and lowest percentages of urban area with decreasing annual Δ EVI were 100% (Kano (Nigeria), Black Corner (Congo) and Lubumbashi (Congo)) and 5.4% (Mbuji-Mayi (Congo)), respectively. Spatially, most cities near the Gulf of Guinea showed percentages of urban area with decreasing annual Δ EVI (19 cities averaged: 79.3%). In addition, the spatial distributions of

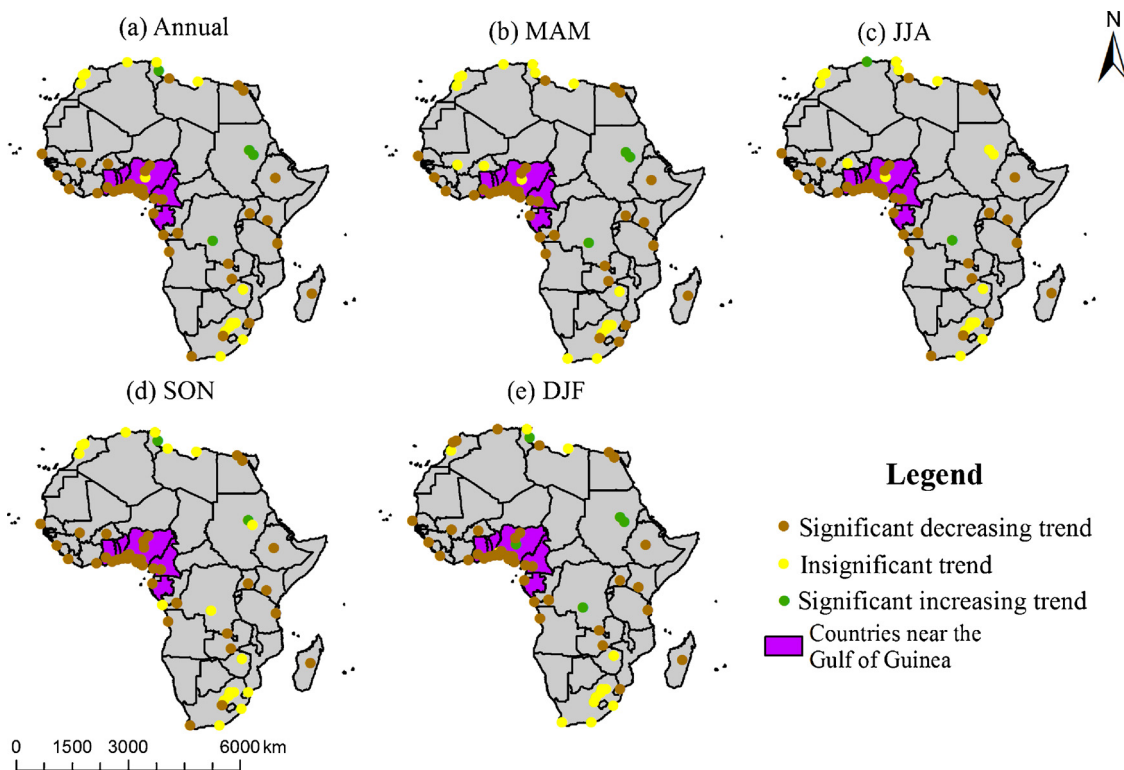


Fig. 6. Spatial distribution of trends of urban EVI in 59 African cities for the period 2001–2017.

percentages of urban area with decreasing Δ EVI differed little by seasons (Table 5). The percentage of urban area with significant increasing, insignificant increasing, insignificant decreasing and significant decreasing Δ EVI from 2001 to 2017.

3.4. Potential consequences of decreased urban EVI

The reductions in VC in urban area may affect human activities and the living environment. Firstly, vegetation can reduce land surface temperature through transpiration. Yao et al. (2017b) showed that the

decreased Δ EVI was an important reason for the increase in surface urban heat island intensity in China for the period 2001–2015. The reductions in Δ EVI may increase the surface urban heat island intensity in Africa. Unfortunately, there are many gaps in the MODIS land surface temperature data in the region near the equator, probably because the continuous cloudy and rainy weather in this region. Thus it is hard to analyze the spatiotemporal variations of surface urban heat island in Africa. Secondly, urban expansion often occupies croplands. Brend d’Amour et al. (2017) showed that urbanization will occupy 1.8–2.4% global cropland by 2030. Thus urbanization may decrease croplands

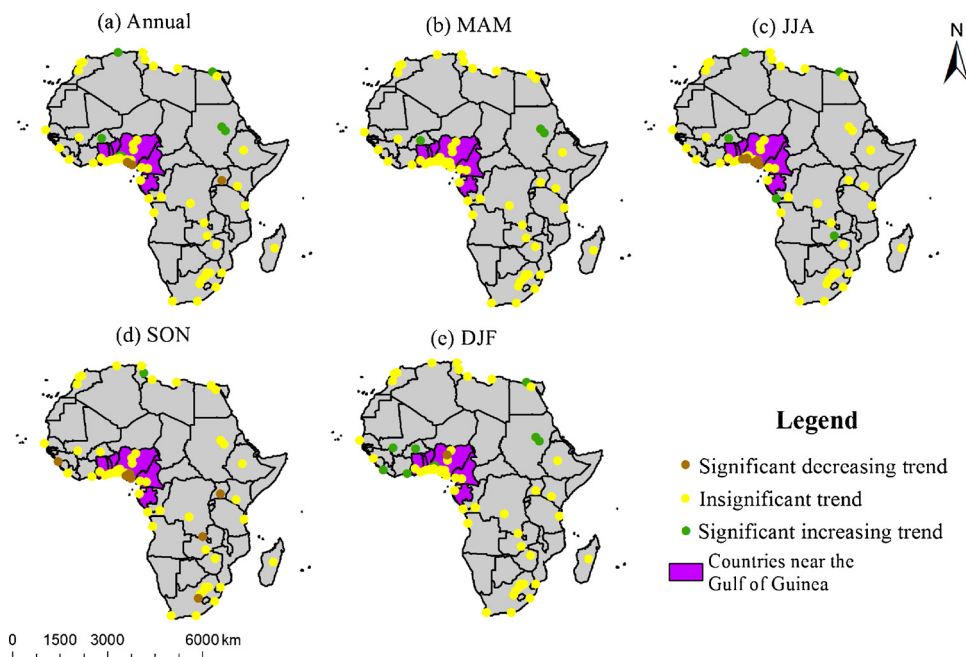


Fig. 7. Spatial distribution of trends of rural EVI in 59 African cities during 2001–2017.

Table 3

Trends of area of urbanization effects on vegetation cover (VC) in 59 African cities from 2001 to 2017. The numbers of cities with increasing and decreasing trends of area of urbanization effects on VC were listed at left and right, respectively. The numbers of cities with significant trends were shown in the brackets.

	Annual	MAM	JJA	SON	DJF
Area of urbanization effects on VC	54(40), 4(1)	54(34), 5(1)	52(34), 7(1)	48(32), 11(2)	53(39), 5(0)

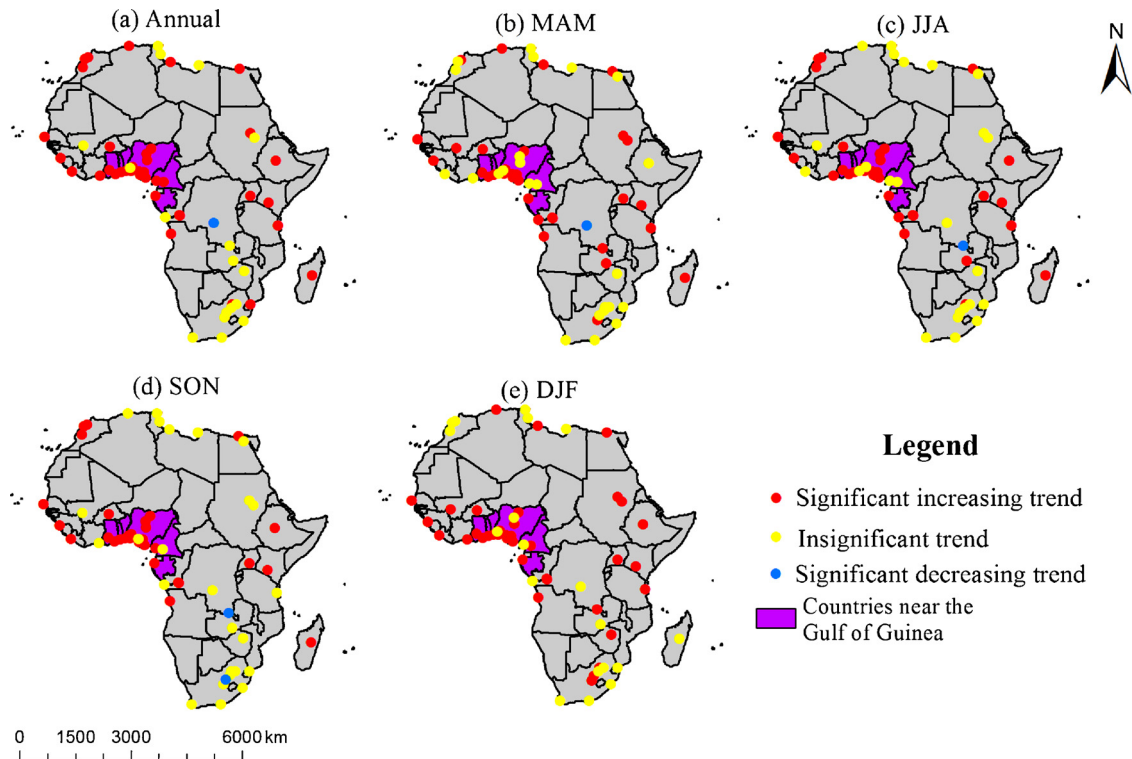


Fig. 8. Spatial distribution of trends of area of urbanization effects on VC in 59 African cities during 2001–2017.

Table 4

Temporal trends of area of urbanization effects on VC averaged for 59 African cities from 2001 to 2017 (Unit: km²).

	Annual	MAM	JJA	SON	DJF
Area of urbanization effects on VC	9.7 ± 9.6	8.9 ± 8.4	8.7 ± 11.1	7.4 ± 9.4	10.3 ± 12.0

and grain output in Africa. Unfortunately, it is well known that the problem of food shortage is more serious in Africa than in other regions (de Waal and Whiteside, 2003; Downing, 1991). Thirdly, Nowak et al. (2006) showed that urban vegetation in the American cities can remove about 711,000 metric tons of air pollutants in a year. Thus the mitigation effects of vegetation on air pollution may decrease in African cities. Thus urbanization and its effects on VC in Africa should arouse more attentions.

3.5. Uncertainties and future works

Note that this study used moderate spatial resolution data (MCD12Q1 and MOD13A3) to analyze urbanization and area of urbanization on VC in 59 African cities. Moderate spatial resolution data is widely used to study urbanization and related environmental impacts for a large area, since it can be processed conveniently and rapidly (Liu et al., 2015; Yao et al., 2017a; Zhou et al., 2014). It is very time consuming to use higher spatial resolution data (e.g. Landsat data) to examine urbanization and area of urbanization on VC for the whole Africa. In addition, higher spatial resolution data generally have lower temporal resolution. However, the accuracy of using moderate

resolution data may be lower than that using higher resolution data. Future studies should use multi-sensor fusion (e.g. Landsat series and MODIS) method to investigate urbanization in a specific city or a small region (e.g. cities near the Gulf of Guinea) in Africa (Cheng et al., 2017; Liu et al., 2017; Shen et al., 2016; Zeng et al., 2013). In addition, the present study showed that urbanization significantly reduced VC in most of the African cities studied. However, the consequence (e.g. increase urban heat island and air pollution, and decrease grain output) of decreased VC remains unclear and should be analyzed in future studies.

4. Conclusions

Urbanization effects on VC were poorly understood in Africa. In this study, MODIS land cover and EVI data were used to reveal urbanization effects on VC in 59 African cities for the period 2001–2017. It was found that: (1) Negative annual Δ EVI (i.e. urban EVI lower than rural) averaged from 2015 to 2017 were observed in 56 of 59 cities. (2) For 59 cities combined, urban area increased 17.9% from 2001 (262.8 km²) to 2016 (309.8 km²). (3) For 59 cities combined, annual Δ EVI decreased at the rate of -0.00268 ± 0.00208 /year for the period 2001–2017. Annual average area of urbanization effects on VC averaged for 59

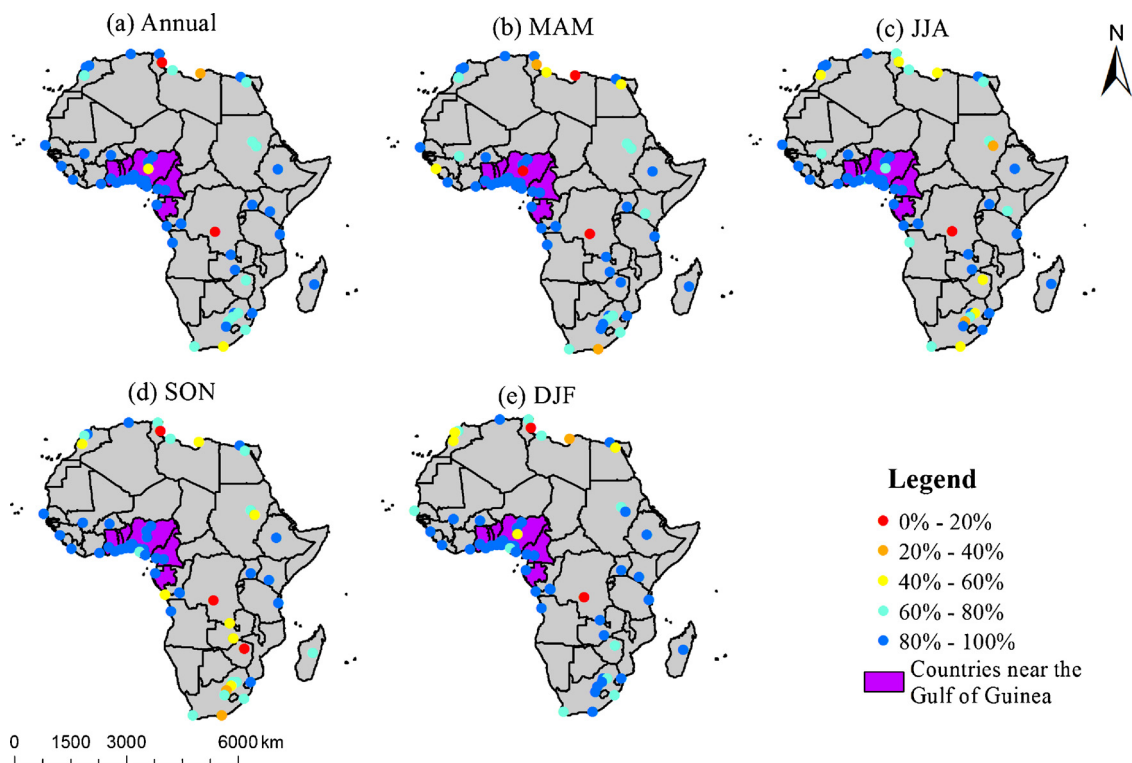


Fig. 9. Spatial distribution of percentage of urban area with decreasing ΔEVI in 59 African cities during 2001–2017.

Table 5
Percentage of urban area with decreasing ΔEVI averaged for 59 African cities for the period.2001–2017.

	Annual	MAM	JJA	SON	DJF
Significant increasing trend	4.6%	3.9%	3.6%	5.2%	3.4%
Insignificant increasing trend	10.6%	15.1%	16.1%	17.3%	12.3%
Insignificant decreasing trend	24.8%	33.8%	39.3%	36.2%	30.3%
Significant decreasing trend	60%	47.2%	41%	41.3%	54.0 %

cities increased at the rate of $9.7 \pm 9.6 \text{ km}^2/\text{year}$. For 59 cities averaged, the percentage of urban area with significant decreasing and increasing trend of annual ΔEVI was 60% and 4.6%, respectively. Cities near the Gulf of Guinea showed more significant decreasing ΔEVI. In addition, the trends and spatial distributions of urbanization effects on VC differed little by seasons.

Overall, for the first time, this study comprehensively investigated urbanization effects on VC in Africa. The results showed that urbanization and its effects on VC in Africa should arouse more attentions. Future studies could: (1) use higher resolution data to analyze urbanization and its effects on VC; (2) examine consequence of decreased VC.

Acknowledgments

This work was financially supported by National Natural Science Foundation of China (No. 41601044), the Special Fund for Basic Scientific Research of Central Colleges, China University of Geosciences, Wuhan (No. CUG150631, CUGL170401 and CUGCJ1704), and Opening Foundation of Key Laboratory for National Geography State Monitoring (National Administration of Surveying, Mapping and Geoinformation). We would like to thank the China Meteorological Administration (CMA) for providing the meteorological and radiation data.

References

Bren d'Amour, C., Reitsma, F., Baiocchi, G., Barthel, S., Guneralp, B., Erb, K.H., Haberl, H., Creutzig, F., Seto, K.C., 2017. Future urban land expansion and implications for global croplands. *Proc. Natl. Acad. Sci. U.S.A.* 114, 8939–8944.

Chen, B., Nie, Z., Chen, Z., Xu, B., 2017. Quantitative estimation of 21st-century urban greenspace changes in Chinese populous cities. *Sci. Total Environ.* 609, 956–965.

Cheng, Q., Liu, H., Shen, H., Wu, P., Zhang, L., 2017. A spatial and temporal nonlocal filter-based data fusion method. *IEEE Trans. Geosci. Remote Sens.* 55, 4476–4488.

Coulter, L.L., Stow, D.A., Tsai, Y.-H., Ibanez, N., Shih, H.-c., Kerr, A., Benza, M., Weeks, J.R., Mensah, F., 2016. Classification and assessment of land cover and land use change in southern Ghana using dense stacks of Landsat 7 ETM+ imagery. *Remote Sens. Environ.* 184, 396–409.

Dallimer, M., Tang, Z., Bibby, P.R., Brindley, P., Gaston, K.J., Davies, Z.G., 2011. Temporal changes in greenspace in a highly urbanized region. *Med. Microbiol. Lett.* 7, 763–766.

Davies, Z.G., Edmondson, J.L., Heinemeyer, A., Leake, J.R., Gaston, K.J., 2011. Mapping an urban ecosystem service: quantifying above-ground carbon storage at a city-wide scale. *J. Appl. Ecol.* 48, 1125–1134.

de Waal, A., Whiteside, A., 2003. New variant famine: AIDS and food crisis in southern Africa. *Lancet* 362, 1234–1237.

Doick, K.J., Peace, A., Hutchings, T.R., 2014. The role of one large greenspace in mitigating London's nocturnal urban heat island. *Sci. Total Environ.* 493, 662–671.

Downing, T., 1991. Vulnerability to hunger in Africa: a climate change perspective. *Glob. Environ. Chang. Part A* 1, 365–380.

Fang, C.-F., Ling, D.-L., 2003. Investigation of the noise reduction provided by tree belts. *Landscape Urban Plan* 63, 187–195.

Foley, J.A., DeFries, R., Asner, G.P., Barford, C., Bonan, G., Carpenter, S.R., et al., 2005. Global consequences of land use. *Science* 309, 570–574.

Han, G., Xu, J., 2013. Land surface phenology and land surface temperature changes along an urban-rural gradient in Yangtze River Delta, china. *Environ. Manage.* 52, 234–249.

Harris, I., Jones, P., Osborn, T., Lister, D., 2014. Updated high-resolution grids of monthly climatic observations—the CRU TS3. 10 dataset. *Int. J. Climatol.* 34 (3), 623–642.

Huete, A., Didan, K., Miura, T., Rodriguez, E.P., Gao, X., Ferreira, L.G., 2002. Overview of the radiometric and biophysical performance of the MODIS vegetation indices. *Remote Sens. Environ.* 83, 195–213.

Liu, X., Shen, H., Yuan, Q., Lu, X., Zhou, C., 2017. A universal destripping framework combining 1-D and 2-D variational optimization methods. *IEEE Trans. Geosci. Remote Sens.* 56, 808–822.

Liu, Y., Wang, Y., Peng, J., Du, Y., Liu, X., Li, S., Zhang, D., 2015. Correlations between urbanization and vegetation degradation across the world's metropolises using DMSP/OLS nighttime light data. *Remote Sens. (Basel)* 7, 2067–2088.

Megahed, Y., Cabral, P., Silva, J., Caetano, M., 2015. Land cover mapping analysis and urban growth modelling using remote sensing techniques in Greater Cairo Region—egypt. *ISPRS Int. J. Geoinf.* 4, 1750–1769.

- Menashe, D.S., Friedl, M.A., 2018. User Guide to Collection 6 MODIS Land Cover (MCD12Q1 and MCD12C1) Product. (accessed 20.05.2018. https://lpdaac.usgs.gov/sites/default/files/public/product_documentation/mcd12_user_user_guide_v6.pdf).
- Myeong, S., Nowak, D.J., Duggin, M.J., 2006. A temporal analysis of urban forest carbon storage using remote sensing. *Remote Sens. Environ.* 101, 277–282.
- Nowak, D.J., Crane, D.E., Stevens, J.C., 2006. Air pollution removal by urban trees and shrubs in the United States. *Urban For. Urban Gree* 4, 115–123.
- Nowak, D.J., Greenfield, E.J., 2012. Tree and impervious cover change in U.S. Cities. *Urban For. Urban Gree* 11, 21–30.
- Nwaogu, C., Okeke, O.J., Fadipe, O.O., Bashiru, K.A., Pechanec, V., 2017. Is Nigeria losing its natural vegetation and landscape? Assessing the landuse-landcover change trajectories and effects in Onitsha using remote sensing and GIS. *Open Geosci* 9.
- Oldfield, E.E., Warren, R.J., Felson, A.J., Bradford, M.A., Bugmann, H., 2013. Challenges and future directions in urban afforestation. *J. Appl. Ecol* n/a-n/a.
- Pathak, V., Tripathi, B.D., Mishra, V.K., 2008. Dynamics of traffic noise in a tropical city Varanasi and its abatement through vegetation. *Environ. Monit. Assess.* 146, 67–75.
- Peng, S., Piao, S., Ciais, P., Friedlingstein, P., Otle, C., Breon, F.M., Nan, H., Zhou, L., Myneni, R.B., 2012. Surface urban heat island across 419 global big cities. *Environ. Sci. Technol.* 46, 696–703.
- Salmund, J.A., Williams, D.E., Laing, G., Kingham, S., Dirks, K., Longley, I., Henshaw, G.S., 2013. The influence of vegetation on the horizontal and vertical distribution of pollutants in a street canyon. *Sci. Total Environ.* 443, 287–298.
- Shen, H., Meng, X., Zhang, L., 2016. An integrated framework for the spatio-Temporal-Spectral fusion of remote sensing images. *IEEE Trans. Geosci. Remote Sens.* 54, 7135–7148.
- United Nations, 2014. World Urbanization Prospects: The 2013 Revision.
- Vitousek, P.M., Mooney, H.A., Lubchenco, J., Melillo, J.M., 1997. Human domination of Earth's ecosystems. *Science*. 277 (5325), 494–499.
- Ward, K., Lauf, S., Kleinschmit, B., Endlicher, W., 2016. Heat waves and urban heat islands in Europe: a review of relevant drivers. *Sci. Total Environ.* 569–570, 527–539.
- Yang, J., Huang, C., Zhang, Z., Wang, L., 2014. The temporal trend of urban green coverage in major Chinese cities between 1990 and 2010. *Urban For. Urban Gree* 13, 19–27.
- Yao, R., Wang, L., Gui, X., Zheng, Y., Zhang, H., Huang, X., 2017a. Urbanization effects on vegetation and Surface Urban Heat Islands in China's Yangtze River Basin. *Remote Sens. (Basel)* 9, 540.
- Yao, R., Wang, L., Huang, X., Chen, J., Li, J., Niu, Z., 2018a. Less sensitive of urban surface to climate variability than rural in Northern China. *Sci. Total Environ.* 628–629, 650–660.
- Yao, R., Wang, L., Huang, X., Niu, Y., Chen, Y., Niu, Z., 2018b. The influence of different data and method on estimating the surface urban heat island intensity. *Ecol. Indic.* 89, 45–55.
- Yao, R., Wang, L., Huang, X., Niu, Z., Liu, F., Wang, Q., 2017b. Temporal trends of surface urban heat islands and associated determinants in major Chinese cities. *Sci. Total Environ.* 609, 742–754.
- Zeng, C., Shen, H., Zhang, L., 2013. Recovering missing pixels for Landsat ETM+ SLC-off imagery using multi-temporal regression analysis and a regularization method. *Remote Sens. Environ.* 131, 182–194.
- Zeng, Z., Piao, S., Li, L.Z.X., Zhou, L., Ciais, P., Wang, T., Li, Y., Lian, X., Wood, E.F., Friedlingstein, P., Mao, J., Estes, L.D., Myneni, Ranga B., Peng, S., Shi, X., Seneviratne, S.I., Wang, Y., 2017. Climate mitigation from vegetation biophysical feedbacks during the past three decades. *Nat. Clim. Change* 7, 432–436.
- Zhang, B., Yang, Y.-s., Zepp, H., 2004a. Effect of vegetation restoration on soil and water erosion and nutrient losses of a severely eroded clayey Plinthudult in southeastern China. *Catena* 57, 77–90.
- Zhang, J., Wang, Y., 2008. Study of the relationships between the spatial extent of surface urban heat islands and urban characteristic factors based on landsat ETM+ data. *Sensors Basel (Basel)* 8, 7453–7468.
- Zhang, X., Friedl, M.A., Schaaf, C.B., Strahler, A.H., Schneider, A., 2004b. The footprint of urban climates on vegetation phenology. *Geophys. Res. Lett.* 31 n/a-n/a.
- Zhang, Y., Song, C., Band, L.E., Sun, G., Li, J., 2017. Reanalysis of global terrestrial vegetation trends from MODIS products: browning or greening? *Remote Sens. Environ.* 191, 145–155.
- Zhao, J., Chen, S., Jiang, B., Ren, Y., Wang, H., Vause, J., Yu, H., 2013. Temporal trend of green space coverage in China and its relationship with urbanization over the last two decades. *Sci. Total Environ.* 442, 455–465.
- Zhou, D., Zhao, S., Liu, S., Zhang, L., 2014. Spatiotemporal trends of terrestrial vegetation activity along the urban development intensity gradient in China's 32 major cities. *Sci. Total Environ.* 488–489, 136–145.
- Zhou, D., Zhao, S., Zhang, L., Liu, S., 2016. Remotely sensed assessment of urbanization effects on vegetation phenology in China's 32 major cities. *Remote Sens. Environ.* 176, 272–281.
- Zhou, W., Wang, J., Cadenasso, M.L., 2017. Effects of the spatial configuration of trees on urban heat mitigation: a comparative study. *Remote Sens. Environ.* 195, 1–12.
- Zhu, Z., Piao, S., Myneni, R.B., Huang, M., Zeng, Z., Canadell, J.G., Ciais, P., Sitch, S., Friedlingstein, P., Arneth, A., Cao, C., Cheng, L., Kato, E., Koven, C., Li, Y., Lian, X., Liu, Y., Liu, R., Mao, J., Pan, Y., Peng, S., Peñuelas, J., Poulter, B., Pugh, T.A.M., Stocker, B.D., Viovy, N., Wang, X., Wang, Y., Xiao, Z., Yang, H., Zaehle, S., Zeng, N., 2016. Greening of the Earth and its drivers. *Nat. Clim. Change* 6, 791–795.